Label-free attomolar detection of lactate based on radio frequency sputtered of nickel oxide thin film field effect transistor

Samira Mansouri Majd, Abdollah Salimi, Bandar Astinchap

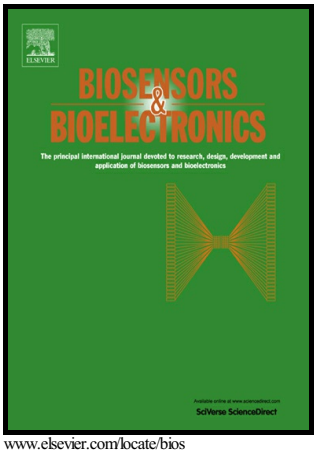

www.elsevier.com/locate/bios

PII: S0956-5663(16)30986-1
DOI: http://dx.doi.org/10.1016/j.bios.2016.09.097
Reference: BIOS9209

To appear in: *Biosensors and Bioelectronic*

Received date: 1 July 2016
Revised date: 16 September 2016
Accepted date: 27 September 2016

Cite this article as: Samira Mansouri Majd, Abdollah Salimi and Banda Astinchap, Label-free attomolar detection of lactate based on radio frequenc sputtered of nickel oxide thin film field effect transistor, *Biosensors an Bioelectronic,* http://dx.doi.org/10.1016/j.bios.2016.09.097

Label-free attomolar detection of lactate based on radio frequency sputtered of nickel oxide thin film field effect transistor

Samira Mansouri Majd[a], Abdollah Salimi[a,b*], Bandar Astinchap[b,c]

[a]Department of Chemistry, University of Kurdistan, 66177-15175, Sanandaj-Iran

[b]Research Center for Nanotechnology, University of Kurdistan, 66177-15175, Sanandaj-Iran

[c]Department of Physics, University of Kurdistan, 66177-15175, Sanandaj-Iran

absalimi@uok.ac.ir

absalimi@yahoo.com

[*]Corresponding author. Tel.: +9887333624001; fax: +9887333624008

Abstract

The radio frequency sputtered nickel oxide thin film nanostructure deposited on glass substrate was used as a potential matrix for the realization of highly sensitive and selective field effect transistor-type lactate biosensor. Firstly, NiO-FET was tested for NADH detection showing a linear concentration range 1aM-1nM and a low detection limit of 0.2 aM. Then, NiO surface modified with chitosan and functionalized with glutaraldehyde and lactate dehydrogenase enzyme was immobilized on the aldehyde terminal. The biosensor is found to exhibit highly efficient sensing response characteristics with good linearity of 1 aM-1 pM and low limit of detection of 0.5 aM. The biosensor shows high stability without interferences from commonly interfering compounds in biological fluids, including uric acid, ascorbic acid, glucose and acetaminophen. Furthermore, the application of the proposed biosensor for analysis of lactate in artificial serum samples was evaluated with good satisfactory results. This

protocol can be used to develop of disposable, low cost, and portable various types of dehydrogenase based biosensor devices using metal oxide nanomaterials.

Keywords: Field effect transistor, Lactate biosensor, NiO thin film, Radio frequency sputtering, Chitosan.

1. Introduction

Developing of improved methods for lactate detection have increased due to its important role in clinical diagnostics, sports medicine, food industry and biotechnology (Azzouzi et al., 2015). Lactate excreted in sweat (Sakharov et al., 2010) and in blood (Loforte et al., 2012) during various physiological and pathophysiological states is a biomarker for a variety of diagnostic purposes, such as hypovolemia, congestive heart failure, liver diseases, metabolic disorders, septic shock, infections, respiratory insufficiency, drug toxicity, mortality in ventilated infants, etc (Chu et al., 2008). Furthermore, lactate is well known as a specific biomarker for specific types of cancers such as prostate and breast cancer (Teseem et al., 2008; Lupo et al., 2010). Pathophysiologic accumulation of lactate has been also associated with a high risk for the formation of metastases and thus with overall low survival chances of cancer patients. Leukocytes may be asphyxiated by the presence of lactate. The differentiation of monocytes to dendritic cells is inhibited by lactate and cytokine release from dendritic cells and cytotoxic T cells (Gottfried et al., 2006) are inactivated. Thus is becomes clear that monitoring of the lactate concentration is important not only for the detection of cancer in its early stage but also during the antitumoral treatment. In addition the increasing of lactate concentration during physical

exercise, making it as useful parameter to monitor wellness, physical fitness and the effects of exercise (Khodagholy et al., 2012). Moreover, lactate in food can indicate the microbial contamination which results in lactate fermentation and lactate levels serve as an indicator of freshness, stability, and storage quality (Gyawali and Ibrahim, 2012). Therefore, development of low cost, simple, rapid, highly sensitive and reliable methods for lactate quantification is considerable.

Several methods for detect of lactate have been proposed, including high-performance liquid chromatography, UV-Vis spectrophotometry, refractive index, electrochemiluminescence, magnetic resonance spectroscopy and electrochemical techniques (Bleiberg et al., 1991; White et al., 2009; Niven et al., 2004; Cai et al., 2010; Yamasaki et al., 2011; Nesakuma et al., 2014, Teymourian et al., 2012). However, these methods are limited by time consuming procedures, use of capital equipment or the rigid nature of the devices, which are unsuitable for a variety of wearable, implantable, real-time, or on-site applications. Thus, the development of sensitive, selective, reliable, high-throughput and label-free, electrochemical detection techniques is now attracting significant attention.

Field-effect transistor (FET) biosensors have the potential to be employed as rapid and low-cost screens for use in label-free electrical detection with the excellent specificity and highly sensitivity. A variety of FET biosensors have been applied for biological detection, such as cell-based FET devices, immunologically modified FET devices, and enzyme-functionalized FET devices (Tran et al., 2016; Chen et al., 2016; Minamiki et al., 2016). Recently, biocompatible nanomaterials, among which the nanostructures based metal oxides semiconductors, such as CuO, SnO_2, ZnO, NiO, TiO_2, and WO_3, have been

increasingly incorporated in biosensing applications and detecting devices, including field effect transistor-based devices (Nehra and Singh, 2015). The fast electron communication, high surface to volume ratios and excellent electrocatalytic effectiveness of metal oxide nanostructures make them suitable matrices for effective immobilization and the desired transducers (Salimi et al., 2007a, Teymourian et al., 2013, Teymourian et al., 2014, Ibupoto et al., 2012, Hallaj et al., 2009, Salimi, et al., 2009, Mansouri Majd, et al., 2013). Among different metal oxides, nickel oxide nanostructures (with band gap 3.6 to 4.0 eV), as natural p-type semiconductor, has recently attracted much attention due to its good sensitivity, low cost, high compatibility with micromachining, high electron transport performance, excellent biocompatibility, high electrocatalytic activity, and photonic and tunable size dependent surface properties (Wang et al., 2015). These unique features of NiO films enabled employing them in various electronic devices such as p-type transparent conducting films, materials for electrochromic display devices, solar cells and as a functional layer material in chemical sensors or biosensors (Salimi et al., 2008, 2007b, Salimi and Roushani, 2005, 2006; Widjonarko et al., 2012; Tsai et al., 2011). Besides being a p-type semiconductor, NiO is also a Mott insulator in which the electronic gap is formed by a charge transfer gap between Ni and O orbitals, even though a strong correlation among electrons exists. FETs that use Mott insulators as a channel material could be of considerable scientific interest because of their different mechanism of gap formation (Zhou et al., 1997; Newns et al., 1998).

NiO nanostructures have been prepared via different deposition techniques, such as chemical vapor deposition, sol-gel, chemical methods, reactive radio frequency sputtering (RF), and plasma-assisted oxidation (Lindahl et al., 2010; Berkat et al., 2005; Chiu et al.,

2005; Varghese et al., 2008) and applied for fabrication of different electrochemical sensors and also as a suitable platform for immobilization of various biomolecules including sRNA, DNA, antibodies and enzymes in biosensors design (Mohan et al., 2011; Ali et al., 2013; Sharifi et al., 2013, 2012, 2014).

Lactate dehydrogenase (LDH) and lactate oxidase are the commonly used enzymes in the development of sensitive lactate biosensor (Ibupoto et al., 2012; Ma et al., 2012; Pratima and Yue, 2013). The successful confinement of lactate dehydrogenase and NAD^+ cofactor onto the electronic transducers could facilitate the development of integrated electrochemical biosensors for lactate. So, developing of novel platform for miniaturized integrated biosensor for lactate detection in vivo is a challenge.

In this study, for the first time we developed a FET based lactate biosensor by immobilizing lactate dehydrogenase (LDH) on the surface of chitosan-modified RF magnetic sputtered nanostructured NiO thin film. In the first step, the application of the proposed NiO-FET for NADH measuring was investigated. By immobilization of LDH onto chitosan modified nickel oxide surface the lactate biosensor was fabricated. The application of the biosensor for lactate measuring at attomolar level was evaluated and interfering of interfering compounds in biological fluids was studied.

2. Experimental

2.1. Reagents and apparatus

NAD^+ (disodium hydrate), NADH, sodium l-lactate (98%) and l-lactate dehydrogenase from rabbit's muscle (LDH, EC 1.1.1.27 140 Umg^{-1}), glutaraldehyde (GA), uric acid (UA), ascorbic acid (AA), glucose (GL), and acetaminophen (AP) were prepared from

Sigma. Chitosan (deacetylated chitin, 85% minimum) was purchased from Merck. Phosphate buffer solutions (PBS, 10mM) with pH 7.4 were prepared with sodium dihydrogen phosphate and disodium hydrogen phosphate and used as supporting electrolyte throughout electrochemical studies. The artificial serum was prepared using the following composition (Merzouk et al., 2014): 8 mmol/L NaH_2PO_4; 1.5 mmol/L Na_2HPO_4; 2.0 mmol/L $CaCl_2$; 0.8 mmol/L $MgCl_2$; 4.5 mmol/L KCl; 0.05 mmol/L NH_4Cl; 4.7 mmol/L glucose; 2.5 mmol/L urea and 0.5 mmol/L urate.

Scanning electron microscopy (SEM) image was obtained with a MIRA3 TESCAN HV: 20.0 KV from Czech Republic. The surface morphologies of the films were measured using an atomic force microscope (AFM, Switzerland, mounted cantilever: noncontact and Operating mode: dynamic force). X-ray diffraction (XRD) patterns were carried out with a Grazing Incidence X-ray Diffraction PHILIPS, model:PW1730. Electrical characteristics of the FETs were measured using a Keithley 2450 Source Meter.

2.2. Fabrication of LDH-Chit-NiO thin film FET biosensor

Fig. 1 shows details regarding the experimental procedures of NiO FET-based lactate biosensor fabrication. The FET based biosensor was fabricated using a facile approach on a glass substrate. After a standard substrate cleaning process of the glass substrate, The sensing layer of nickel oxide is first deposited on a glass substrate by using RF reactive magnetron sputtering technique with a 2 in. diameter metallic nickel (Ni) target (99.99% pure). The sputtering was done under a the total gas pressure of 2×10^{-2} mbar of a mixed atmosphere of oxygen (50%) and argon (50%) and the RF power is maintained at 100W (a). Next, Au (with 30 nm thickness) source and drain electrodes were deposited on the NiO thin film by RF sputtering

technique and using of a mask. The channel width and length were 5 and 1 mm, respectively (b). Then, the electrodes were covered with a silicone adhesive sealant to reduce the contact area between the electrodes and the electrolyte (c). The surface of NiO thin film was treated with optimized 0.5 wt % chitosan solution (acetate buffer, 0.05 M, pH 4.2) for 1 h (Fig. S1) (d). Chitosan (Chit) was immobilized on the surface of NiO thin film through electrostatic interactions between the hydroxy group of chitosan with NiO and also because of complex formation Chit molecules with NiO thin film surface (Solanki et al., 2015). The resulting Chit-immobilized substrate was rinsed with distilled water. LDH enzyme was immobilized onto chitosan modified NiO film through imine bond formation between the amino groups of LDH and chitosan. Thus, 2.5 % glutaraldehyde solution (10 μL) was spread onto Chit-NiO surface via drop casting for 1 h (e) and then the modified surface exposed to 10% wt LDH solution (10 μL) for 2 h (f). Subsequently, the substrate was rinsed with distilled water and was stored at 4°C when not in use.

2.3. Electrical measurements

Phosphate buffered solution (PBS) (pH 7.4) was used as a liquid-ion gate for FET lactate biosensor. A solution chamber (volume 10 µL of PBS) containing 1 nM of NAD^+ and different concentrations of lactate was designed and employed for all solution-based measurements. The Ag/AgCl reference electrode immersed in 10mM PBS was used as gate electrode. All electrical measurements were conducted with a Keithley 2450 Source Meter. In order to characterize the charge transport properties of LDH-Chit-NiO thin film in the FET configuration, the dependence of the drain-source current (I_{DS}) versus drain-source voltage (V_{DS}) was investigated at a constant gate voltage (V_G). All electrical measurements were performed at optimized room temperature (Fig. S2).

3. Results and discussion

3.1. Characterization

X-ray diffraction (XRD) was used to investigate crystallographic structure of deposited NiO nanostructure layer on glass substrate (Fig. 2a). Broad peak appeared at 2θ of about 22° is related to glass substrate and two peaks observed at 2θ=36.78° and 42.83° are attributed to the crystal planes with miller indices of (111) and (200), respectively, and they are in good agreement with the standard X-ray diffraction data of pure cubic NiO (JCPDS 47-1049). The ellipsometry analysis indicated that the deposited NiO film had a thickness of 60 nm. The surface of nanostructure NiO thin film was analyzed via scanning electron microscopy (SEM) (Fig. 2b). The SEM image of the NiO thin film confirmed the layered-island growth of thin film and the formation of a nanoporous and dense morphology. This uniform and highly ordered porous morphology is expected to lead to a higher surface area and thus providing more surface sites available for modification and adsorption of NADH and improving the sensitivity of the sensor. AFM images of the surface of NiO thin film (Fig. 2c) and LDH immobilized NiO surface (Fig. 2d) further corroborate the FESEM results. Roughness of the film surface (average root measure roughness), an important parameter for sensing applications that plays a major role in the charge transfer capacity calculated using SPM Lab Analysis software, is about 380.01 pm for the NiO thin film. AFM micrograph of LDH immobilized biosensor (LDH-Chit-NiO) shows the uniformly distributed globular structure along with an increase in its average rms surface roughness to 1978.1 pm indicating successful immobilization of LDH on the surface of NiO thin film. Fig. S3 shows the 3-dimensional view of the respective images. The elemental composition of the NiO thin film were analyzed via energy dispersive X-

ray spectroscopy (EDX) (Fig. S4). The thickness of the sensing layer plays an important role for the sensitivity of the biosensor. We used four thicknesses for NiO thin film. The ellipsometry analyses indicated that the deposited NiO film had the thickness of 5, 21.8, 31.5 and 60 nm. Our experiments revealed that the thicker samples had dI_{DS}/dV_{DS} higher than the thinner samples when they were exposed to 1nM of lactate. Thus, we used 60 nm-thick sample as optimized thickness for our experiments.

These results indicate, the growth and formation of thin film are very important factors in electron transfer on surface of thin film and for the thickness of lower than 30 nm, the NiO nanostructure has island growth on the substrate and film formation is not complete. Thus electron transfer in longitude of the thin film is slow and the NiO nanostructures form layered thin film structure with increasing of the film thickness from 21.8 nm to 60 nm. As a result, electron transfer becomes faster in longitude of the uniform thin film and maximum current are obtained. Furthermore, as reported in literature (Chen et al., 2006), the nickel oxide thin films were deposited by RF with the lowest resistance could be obtained in the condition of substrate unheated with a film of 200 nm thickness.

3.2. Electrical properties

The fabrication of the device at each step of surface modification was monitored by recording the drain-source current-voltage (I_{DS}-V_{DS}) characteristics (Fig. 3a). Linear I_{DS}-V_{DS} curves were observed over a range of 0.0 V to +0.5 V, indicating that Ohmic contacts were formed between the nanocomposites and the gold electrodes. As can be seen a decrease in the slope (i.e., dI_{DS}/dV_{DS}) was observed after each step (Fig. 3a, inset table). Moreover, after enzyme immobilization, the linearity in I_{DS}-V_{DS} characteristics was

preserved and the dI_{DS}/dV_{DS} values were also maintained within the same order of magnitude. Therefore, it can be considered that enzyme molecules are effectively immobilized on the NiO thin film without any deterioration in electrical contact and conductivity. To investigate the electrical characteristics of the NiO thin film conductive channel, we measured the drain-source current-voltage characteristics of NiO thin film FET under various gate biases (Fig. 3b) and the drain-source current versus gate voltage at constant drain-source voltage (1.0 V) (Fig. S5). For the former measurements, the I_{DS}-V_{DS} curves of biosensor at different biases of V_G from -20 to 0.0 V in 5 V steps (V_{SD}: -2 to 2 V) was recorded. The increasing I_{DS} with decreasing V_G is a typical characteristic of p-channel transistors and therefore we conclude that the current in the device was due to hole transport and that the modulation of I_{DS} resulted from control over the hole carrier density at the surface of NiO thin film (Matsubara et al., 2014; Shimotani et al., 2008).

Fig. 4a schematically depicts an enzyme FET biosensor platform based on LDH-Chit-NiO thin film. To study the response of the proposed solution-gated NiO thin film FET biosensor, the dI_{DS}/dV_{DS} value was measured in the absence and presence of 1 pM solution of lactate in the presence of 1nM NAD^+ at a fixed gate voltage (V_G=-0.1 V) provided through an Ag/AgCl reference electrode. As shown in inset of Fig. 4a, the current value substantially decreases after lactate addition compared to condition free of it. This decrease in the current response is considered due to the formation of NADH in the following enzymatic reaction:

$$\text{Lactate} + NAD^+ \xrightarrow{LDH} \text{Pyruvate} + NADH + H^+ \quad (1)$$

$$NADH \rightarrow NAD^+ + H^+ + 2e^- \quad (2)$$

Enzyme LDH catalyzes the oxidation of lactate while the cofactor NAD^+ get reduced to dihydronicotinamide adenine dinucleotide (NADH). The NADH generated in the enzymatic reaction is oxidized at the surface of NiO nanostructure. Since the concentrations of NAD^+ and its oxidation products are constant, the decrease in the electrocatalytic current only depends on the lactate concentration. Fig. 4b shows the lactate biosensing protocol using the LDH-Chit-NiO thin film platform. In NiO, a typical Mott insulator, the electronic gap is formed by a charge transfer gap between Ni and O orbitals, even though a strong correlation among electrons exists. Oxidation state of Ni in NiO is same as the formal Ni (d^8) that is two holes per Ni atom. These d^8 holes are mobile because metal-insulator transition (Matt transition) occurs and the system goes from an insulating to a metallic state. However, as more holes are added, they combine with the d^8 holes to form a fully mobile hole gas with metallic character and the conductivity becomes a high, metallic one (Zhou et al., 1997; Newns et al., 1998; Hufner, 2010). The electrons generated from the oxidation of NADH on the surface of NiO nanostructure discharge into the d^8 orbitals and decrease the I_{DS} in the p-type conductor sheet at the interface of NiO nanostructure and the solution. In this system, NiO nanostructure acts as a strong electrocatalyst for NADH oxidation.

The electrochemical oxidation of NADH to the corresponding oxidized form (NAD^+) in aqueous solution has received considerable interest, owing to its significance both as a substrate for dehydrogenase enzymes and also to the design of the novel biosensors, because NAD^+/NADH dependent dehydrogenases constitute the largest group of redox enzymes known today (Bartlett et al., 2002). Thus, at first, we characterized the real-time response of the NiO nanostructure FET biosensor toward various concentration of

NADH. Fig.4c shows the plotted of I_{DS} against V_{DS} for various concentrations of NADH at a fixed reference voltage of -0.1V. The sensor response displayed linear concentration range from (1 aM-1nM) with a correlation coefficient of 0.9917 and the detection limit of 0.2aM (S/N = 3).

3.3. Sensitivity of the biosensor toward NADH and lactate

The sensitivity was determined from change in the normal conductance $\Delta g_{DS}/g_0 = (g_{DS} - g_0)/ g_0$, where g_0 and g_{DS} are the values for conductance of device measured before and after exposure to analyte in PBS, respectively. The conductance was calculated as the slope of the I_{DS}-V_{DS} plot between 0.0 and 0.5V. The device was exposed to 10 µl aliquot of each concentration of NADH for 15 s, at room temperature. It was observed that the conductance of the device continued to decrease with increasing concentrations of NADH due to decrease in the concentration of charge carriers (holes) (Fig. 4d). The fabricated NiO nanostructure FET biosensor shows linearity with a high regression coefficient (R^2) value of 0.9917. Error bars show a standard deviation of 3.5% for three different electrodes.

Furthermore, to understand the sensing performance of the LDH-Chit-NiO nanostructure FET biosensor, different concentrations of lactate (LA) were prepared in 10 mM PBS (pH = 7.4) in the presence of 1nM NAD^+ and the device charge transfer characteristics were recorded (Fig 5a). As illustrated in Fig. 5b, very good linear dependence between changes of biosensor conductivity and lactate concentration at the wide range (1aM-1pM). The R^2 of the linear regression is 0.9947, indicating a high degree of accuracy throughout the assay range. The limit of detection was calculated based on the standard deviation of response and the slope of the calibration curve, and it

was 0.5 aM (S/N=3). The analytical characteristic of the LDH-Chit-NiO thin film FET lactate biosensor is substantially improved compared to other lactate biosensors (Table 1). These results indicate that the proposed FET sensor is effectively able to monitor the very low concentration of produced lactate at enzymatic reaction.

3.4. Reproducibility, storage stability and selectivity

The reproducibility and storage stability of the proposed FET lactate system were also evaluated. To investigate the reproducibility, four devices were fabricated and their measuring experiments for 5 pM of lactate were performed. The biosensor showed response with a relative standard deviation of 3.6%. Furthermore, coefficient variation of the sensor was 3.5% for 6 repeated measuring of 5 pM lactate. Storage stability of the presented biosensor was assessed in ambient condition and after 3 weeks of storage, the FET biosensor retains about 94% of its original response for picomolar concentration of lactate. The small decrease in response is probably due to a slight loss in stability of immobilized enzyme. These results indicate acceptable reproducibility and stability of the proposed lactate biosensor. Furthermore, to show an index of biosensor stability we recorded time-dependent response of 1pM lactate over a continuous period of 1000 seconds. The current reaches to maximum during about 15s and after 1000 seconds the current decreases to 82 % of the initial response.

The selectivity of the biosensor toward lactate was evaluated by measuring the response of the proposed FET for various interfering species commonly found in biological fluids, including uric acid (UA), ascorbic acid (AA), glucose (GL) and acetaminophen (AP) compared to lactate (Fig. 5c), when their concentrations changed from 10 aM to 1pM in PBS at constant V_G of -0.1V. Although the response of the device was found to decrease with increasing concentration of interfering species, but changes in response were

significantly smaller in comparison to response change for the same concentration range of lactate. Furthermore, as can be seen in recorded chart bars in Fig. 5d, the change in measured response for 1pM of each interfering species compared to 1pM lactate is not significant. These results clearly demonstrate the specificity of the proposed FET based biosensor toward lactate.

3.5. Detection of lactate in artificial serum

In order to estimate the applicability of the methodology, the proposed lactate biosensor was applied to the measurement of lactate concentration in artificial serum. Therefore, in order to estimate the response of biosensor in a real sample, we have prepared an artificial serum containing the most common compounds of the real serum with its corresponding concentrations (Azzouzi et al., 2015). The normal lactate concentration in human serum ranges between 0.5 mM-1.5 mM (Rassaei et al., 2013). The normal therapeutic range of ascorbate is between 0.03 mM to 0.11 mM. Therefore, taking also into consideration the increase of the lactate concentration in the case of a cancer tumor, the ratio of [lactate]/[ascorbate] is higher than 10. Next, we have measured the I_{DS} in the presence and in absence of 0.1 mM ascorbic acid in the artificial serum after adding of 1 mM lactate and dilution of the samples to 1pM of lactate (Fig. S5a, b). Based on the obtained data, the calculated concentration of lactate was 0.96(± 0.03) pM. Furthermore, after three individual measurements the conductance decreased from 2.68 ± 0.24 µS in absence of ascorbate to 2.72 ± 0.06 µS in presence of 0.1 mM ascorbate. However, this decrease falls well within the limits of experimental error. It thus can be concluded that the detection of lactate in serum samples by LDH-Chit-NiO thin film is not affected by the presence of ascorbic acid and uric acid at physiological level. The biosensor we have developed in this work can be successfully used for detection of lactate as tumor biomarker in biological samples.

4. Conclusion

In summary, we developed a highly sensitive and selective lactate biosensor based on RF sputtered NiO nanostructure FET. The NiO-FET has been tested for NADH detection at linear concentration range of 1aM-1nM with low detection limit of 0.2 aM. Due to excellent electron transfer capabilities besides high adsorption ability and electrocatalytic activity of the NiO nanostructure, it can be applied as an efficient transducer in the design of biosensors based on coupled dehydrogenase enzymes, using LDH as a model enzyme. The FET based biosensor devices exhibited a novel strategy for lactate at attomolar level sensitivity and a linear dynamic range 1aM-1pM with offering a low limit of detection of 0.5 aM. Furthermore, the application of the proposed sensor for lactate detection in artificial serum samples was successfully demonstrated. These encouraging results with high reproducibility, long time stability, low cost and easy of fabrication promising this protocol for developing of disposable dehydrogenase based biosensors.

Acknowledgements
This research was supported by the Iranian Nanotechnology Initiative and the Research Offices of the University of Kurdistan.

References

Ali, M. A., Srivastava, S., Solanki, P. R., Reddy, V., Agrawal, V. V., Kim, C., John, R., Malhotra, B. D., 2013. Scientific reports 3, 1-9.

Azzouzi, S., Rotariu, L., Benito, A.M., Maser, W.K., Ben Ali, M., Bala, C., 2015, Biosens. Bioelectron. 69, 280-286.

Bartlett, P.N., Simon, E., Toh, C.S., 2002. Bioelectrochemistry 56, 117-122.

Berkat, L., Cattin, L., Reguig, A., Regragui, M., Bernede, J. C., 2005. Mater Chem Phys. 89, 11-20.

Bleiberg, B., Steinberg, J.J., Katz, S.D., Wexler, J., Lejemtel, T., 1991. J. Chromatog. B 568, 301-308.

Cai, X., Yan, J. L., Chu, H. H., Wu, M. S., Tu, Y. F., 2010. Sens. Actuators, B. 143, 655-659.

Chen, H., Chen, P., Huang, J., Selegard, R., Platt, M., Palaniappan, A., Aili, D., Tok, A. Y., Liedberg, B., 2016. Anal. Chem. 88, 2994-2998.

Chen, H-L., Lu, Y-M., Hwang, W-S., 2006. Thin Solid Films 498, 266-270.

Chiu, K. F., Chang, C. Y., Lin, C. M., 2005. J. Electrochem. Soc. 152, A1188-1192.

Chu, B. H., Kang, B. S., Ren, F., Chang, C. Y., Wang, Y. L., Pearton, S. J., Glushakov, A. V., Dennis, D. M., Johnson, J. W., Rajagopal, P., Roberts, J. C., Piner, E. L., Linthicum, K., 2008. J. Appl. Phys. Lett. 93, 042114-3.

Gottfried, E., Kunz-Schughart, L.A., Ebner, S., Muelle -Klieser, W., Hoves, S., Andreesen, R., Mackensen, A., Kreutz, M., 2006. Blood 107(5), 2013-2021.

Gyawali, R., Ibrahim, S., Emirates, A., 2012. J. Food Agricult. 24, 1-11.

Hallaj, R., Salimi, A., Akhtari, K., Soltanian, S., Mamkhezri, H., 2009, Sens. Actuators B. 135,632-641.

Hufner, B. S., Adv. Phys., 1994, 43, 183-356.

Ibupoto, Z.H., Shah, S.M.U.A., Khun, K., Willander, M., 2012. Sensors 12, 2456-2466.

Khodagholy, D. V., Curto, F., Fraser, K. J., Gurfinkel, M., Byrne, R., Diamond, D., Malliaras, G. G., Benito-Lopez, F., Owens, R. M., 2012. J. Mater. Chem. 22, 4440-4443.

Lindahl, E., Ottosson, M., Carlsson, J.O., 2010. Surf. Coat. Technol. 205, 710-716.

Loforte, A., Montalto, A., Ranocchi, F, Della Monica, P.L., Casali, G., Lappa, A., Menichetti, A., Contento, C., Musumeci, F., 2012. Artificial Organs 36, E53-E61.

Lupo, J.M., Chen, A.P., Zierhut, M.L., Bok, R.A., Cunningham, C.H., Kurhanewicz, J., Vigneron, D.B., Nelson, S.J., 2010. Magn. Reson. Imaging 28 (2), 153-162.

Ma, S., Liao, Q., Liu, H., Song, Y., Li, P., Huang, Y., Zhang, Y., 2012. Nanoscale 4, 6415-6418.

Mansouri Majd, S., Teymourian, H., Salimi, A., Hallaj, R., 2013. Electrochim. Acta 108, 707- 716.

Matsubara, K., Huang, S., Iwamotob, M., Pan, W., 2014. Nanoscale 6, 688-692.

Merzouk, S., Zine, N., Agouzoul, M., Janan, M.-T., Bausells, J., Teixidor, F., Jaffrezic-Renault, N., Errachid, A., 2014. Sens. Transducers J. 27, 258-263.

Minami, T., Sato, T., Minamiki, T., Fukuda, K., Kumaki, D., Tokito, S., 2015. Biosens. Bioelectron. 74, 45-48.

Minamiki, T., Minami, T., Koutnik, P., Anzenbacher, P., Tokito, S., 2016. Anal. Chem. 88, 1092-1095.

Mohan, S., Srivastava, P., Maheshwari, S., Sundar, S., Prakash, R., 2011. Analyst 136, 2845-2851.

Nehra, A., Singh, K. P., 2015. Biosens. Bioelectron. 74, 731-743.

Nesakumar, N., Thandavan, K., Sethuraman, S., Krishnan, U. M., Rayappan, J. B. B., 2014. J. Colloid Interface Sci. 414, 90-96.

Newns, D. M., Misewich, J. A., Tsuei, C. C., Gupta, A., Scott, B. A., Scott, A., 1998. Appl. Phys. Lett. 73, 780-782.

Niven, S.J., Beal, J.D., Brooks, P.H., 2004. Anim. Feed Sci. Technol. 117, 339-345.

Pratima, L., Yue, C., 2013. Biosens. Bioelectron. 41, 852-856.

Rassaei, L., Olthuis, W., Tsujimura, S., Sudhölter, E.J.R., Van Den Berg, A., 2013. Anal. Bioanal. Chem. 406(1), 123-137.

Sakharov, D.A., Shkurnikov, M.U., Vagin, M.Y., Yashina, E.I., Karyakin, A.A., Tonevitsky, A.G., 2010. Bull. Experimen. Biol. Med. 150, 83-85.

Shimotani, H., Suzuki. H., Ueno, K., Kawasaki, M., Iwasa, Y. 2008. Appl. Phys. Lett. 92, 242107-3.

Salimi, A., Hallaj, R., Soltanian, S.,2007a. Biophys. Chem. 130 , 122-131.

Salimi, A., Hallaj, R., Soltanian, S. , 2009. Electroanalysis 21, 2693 -2700

Salimi, A , Sharifi, E., Noorbakhash, A., Soltanian, S., 2007b. Biosens. Bioelectron. 22 , 3146-3153.

Salimi, A , Roushani, M., Hallaj, R., Soltanian, S., 2007. Anal. Chem. 79,7431‑7438.

Salimi, A , Roushani, M., 2005. Electrochem. Commun. 7 , 879-887.

Salimi, A , Roushani, M., 2006. Electroanalysis 18, 2129–2136.

Sharifi, E., Salimi, A., Shams, E., 2012. Bioelectrochemistry 86, 9-21.

Sharifi, E., Salimi, A., Shams, E., Noorbakhash, A., Amini, M.K.,2014. Biosens. Bioelectron. 56, 313-319.

Sharifi, E., Salimi, A., Shams, E., 2013. Biosen. Bioelectron. 45, 260-266.

Solanki, P. R., Patel, M. K., Ali, M. d. A., Malhotra, B. D., 2015. J. Mater. Chem. B 3, 6698-6708.

Teymourian, H., Salimi, A., Hallaj, R., 2012. Biosens. Bioelectron. 33, 60- 68.

Teymourian, H., Salimi, A., Khezrian, S., 2013. Biosens. Bioelectron.49, 1-8.

Teymourian, H., Salimi, A., Firoozi, S., Korani, A., Soltanian, S.,2014. Electrochim. Acta 143 196-206.

Tran, D. P., Winter, M. A., Wolfrum, B., Stockmann, R., Yang, C-T., Pourhassan-Moghaddam, M., Offenha user, A., Thierry, B., 2016. ACS Nano 10, 2357-2364.

Tsai, S.Y., Hon, M. H., Lu, Y. M., 2011. Solid-State Electronics 63, 37-41.

Varghese, B., Reddy, M. V., Yanwu, Z., Lit, C. S., Hoong, T. C., Rao, G. V. S., 2008. Chem. Mater. 20, 3360-3367.

Wang, J., Yang, P., Wei, X., Zhou, Z., 2015. Nanoscale Res. Lett. 10, 119-124.

White, R., Yaeger, D., Stavrianeas, S., 2009. Int. J. Exerc. Sci. 2, 83-93.

Widjonarko, N. E., Ratcliff, E. L., Perkins, C. L., Sigdel, A. K., Zakutayev, A., Ndione, P. F., Gillaspie, D. T., Ginley, D. S., Olson, D. C., Berry, J. J., 2012. Thin Solid Films 520, 3813-3818.

Xu, J. J., Zhao, W., Luo, X. L., Chen, H. Y., 2005. Chem. Commun. 792-794.

Yamasaki, F., Kurisu, K., Kajiwara, Y., Watanabe, Y., Takayasu, T., Akiyama, Y., Saito, T., Hanaya, R., Sugiyama, K., 2011. Neuro-Oncology 13, 791-801.

Zhou, C., Newns, D. M., Misewich, J. A., Pattnaik, P. C., 1997. Appl. Phys. Lett. 70, 598-600.

Fig. 1 Schematic illustration for fabrication of LDH-Chit-NiO thin film FET biosensor: (a) RF reactive magnetron sputtering of NiO thin film, (b) RF sputtering of Au source and drain electrodes on the NiO thin film, (c) cover of electrodes with a silicone adhesive sealant (d) drop casting of chitosan solution, (e) drop casting of glutaraldehyde solution onto Chit-NiO surface and (f) the exposing of modified surface to LDH solution.

Fig. 2 (a) XRD of deposited NiO nanostructure layer on glass substrate. (b) SEM of NiO thin film FET biosensor before enzyme immobilization. AFM images of NiO thin film FET biosensor before (c) and after (d) modification with LDH-Chit.

Fig. 3 (a) I_{DS}-V_{DS} characteristics of FET biosensor at different modification steps consist of NiO, Chit-NiO, GA-Chit-NiO and LDH-GA-Chit-NiO. Table shows dI_{DS}/dV_{DS} at each step (Inset). (b) (b.)I_{DS}-V_{DS} curves of biosensor at different biases of V_G from -20 to 0 V in 5 V steps (V_{SD}: -2 to 2 V)

Fig. 4 (a) A FET sensor configuration with PBS (pH 7.4) as a liquid-ion gate. The inset shows I_{DS}-V_{DS} characterization of biosensor before "a" and after "b" lactate insertion (1pM) in presence of 1nM NAD^+ at V_G=-0.1 V. (b) the lactate biosensing protocol using the LDH-Chit-NiO thin film platform. (c) I_{DS}-V_{DS} responses with increasing NADH concentration (1 aM–1 nM) and (d)

their corresponding calibration curve, i.e. percentage of normalized change in the conductance vs. NADH concentration (C) in log scale.

Fig. 5 (a) I_{DS}-V_{DS} responses with increasing lactate concentration (1 aM-1 pM) in PBS (pH 7.4) in presence of 1nM NAD^+ at V_G= -0.1 V and their corresponding calibration curve (b). (c) I_{DS}-V_{DS} responses with increasing uric acid, acetaminophen, ascorbic acid and glucose concentration from 10 aM to 1 pM in PBS at V_G= -0.1 V. (d) A histogram details the sensing performance of the LDH-Chit-NiO thin film FET biosensor to 1pM lactate, uric acid, acetaminophen, ascorbic acid and glucose at V_G=-0.1 V.

Table 1. Analytical characteristics of different FET based biosensors for lactate detection

Biosensor configuration	Detection limit	Linear range (µM)	Sensitivity	Response time
LOx-ZnO NR-gated AlGaN/GaN HEMT (Chu et al., 2008)	167 nM	167 nM-139 µM.	-	~20s
LOx-Fc- PEDOT:PSS- OECT (Khodagholy et al., 2012)	10mM	10–100 mM	-	~10 min
LDH-NAD+-PQQ ENFET (Kharitonov et al., 2001)	0.1mM	0.1 -10 mM	24±2mV dec^{-1}	15 s
LDH-PAA-Si_3N_4 FET (Lupu et al., 2007)	0.2µM	0.2-10 µM-	49.7mV dec^{-1}	~50 s
LOx-ZnO NWs-gated AlGaAs/GaAs HEMT (Ma et al., 2012)	0.03nM	0.03 nM-300 mM	-	~1s
LOx-graphene flexible substrate FET (Pratima et al., 2013)	0.08 µM	0.08 µM -20 µM	29.869.0nA $µM^{-1}$	2s
LOx-HRP-Os-Au extended-gate OFET (Minami et al., 2015)	66 nM	0–1000nM	-	~50 s
$(PDDA/MnO_2/PDDA/LOx)_3$ ENFET (Xu et al., 2005)	8µM	0.1mM-5mM	16.84 mV mM^{-1}	~50 s
LDH-Chit-NiO FET (this study)	1aM	1aM-1pM	-	~15s

LOx: lactate oxidase enzyme, NR: nanorod, HEMT: high electron mobility transistor, Fc: Ferrocene, PEDOT:PSS: poly(3,4-ethylenedioxythiophene) doped with poly(styrene sulfonate), OECT: organic electrochemical transistor, LDH: lactate

dehydrogenase, NAD^+: nicotinamide dehydrogenase, PQQ: Pyrroloquinoline quinone, ENFET: enzyme field effect transistor, PAA: polyacrylic acid, NWs:nanowires, HRP: horseradish peroxidase, Os: osmium redox polymer, OFET: organic field effect transistor, PDDA: poly(dimethyldiallylammonium chloride).

Highlights

- The radio frequency sputtered NiOX thin film deposited on glass substrate
- NiOx film used as electrochemical platform for FET-sensor toward NADH detection
- With immobilizing of LDH, a novel biosensor for aM detection of lactate fabricated
- FET device used for selective detection of lactate in the presence of interferences
- The protocol promised for fabrication disposable dehydrogenase based biosensors

Graphical Abstract

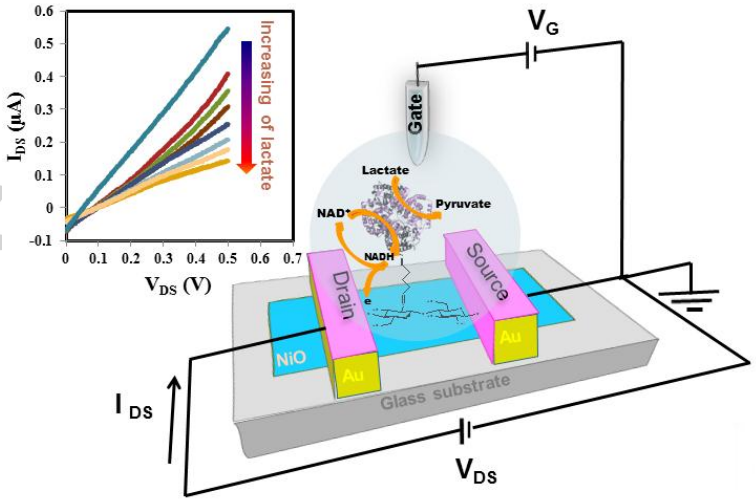

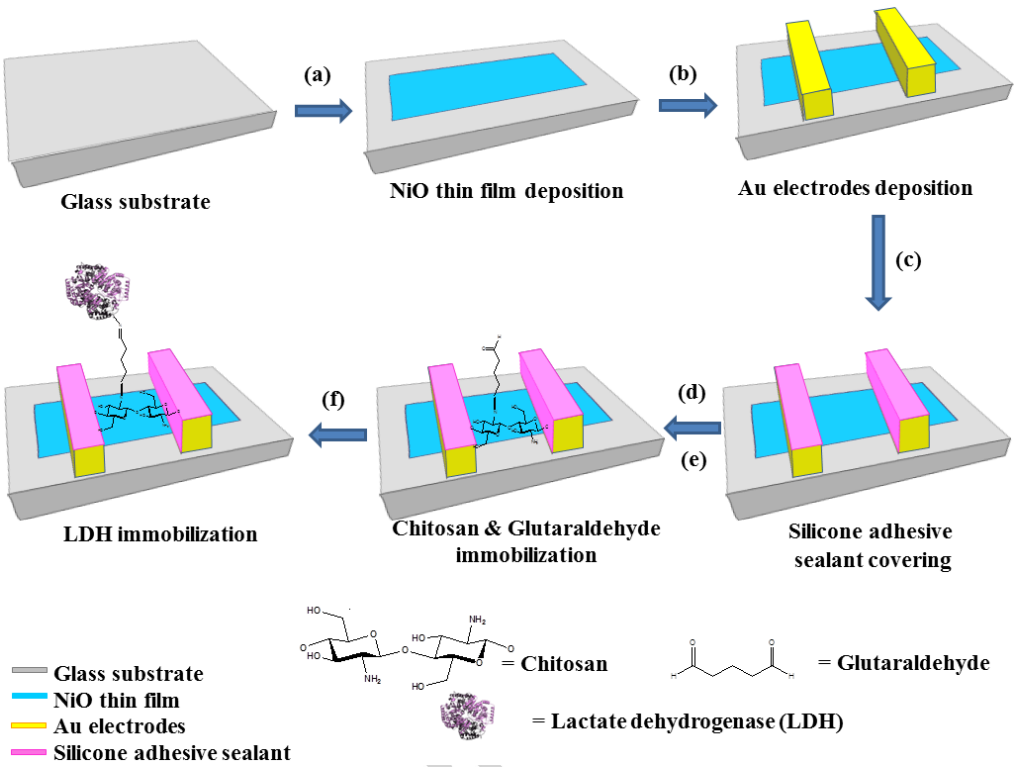

Fig.1

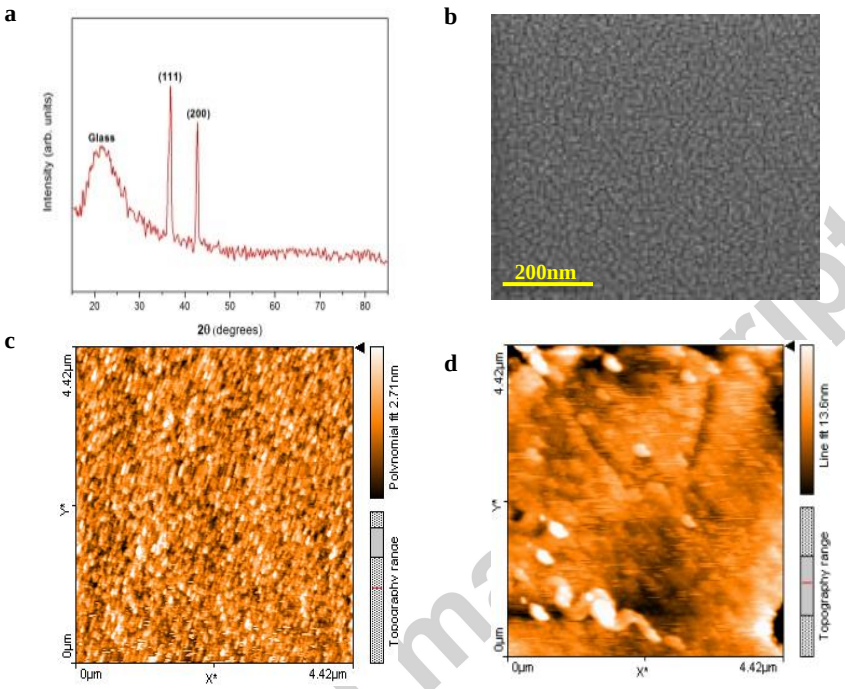

Fig.2

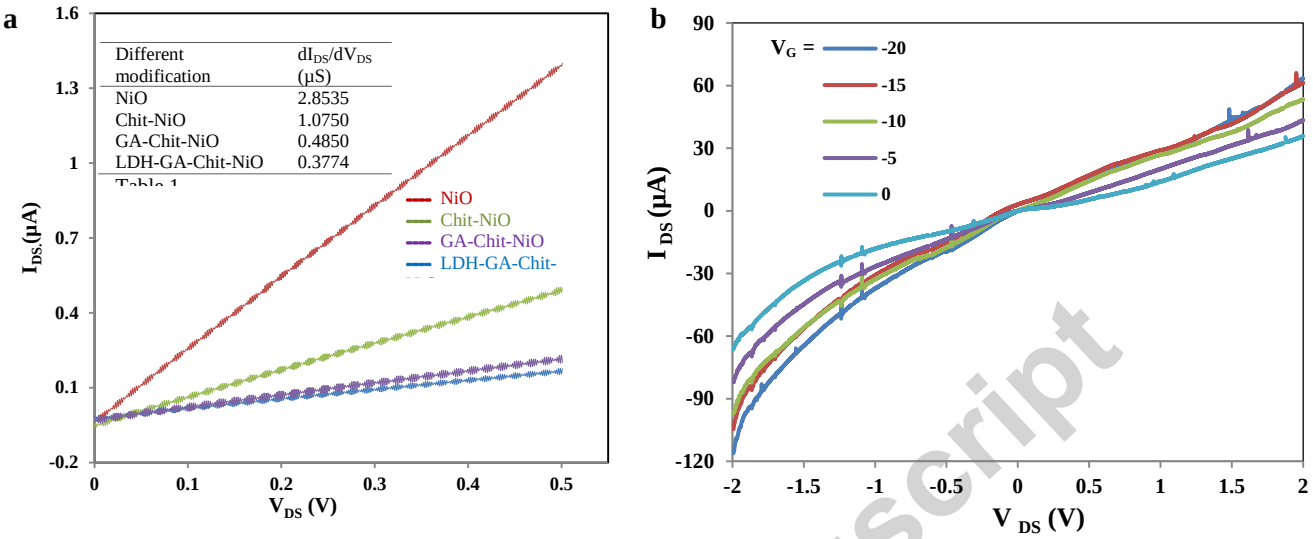

Fig. 3

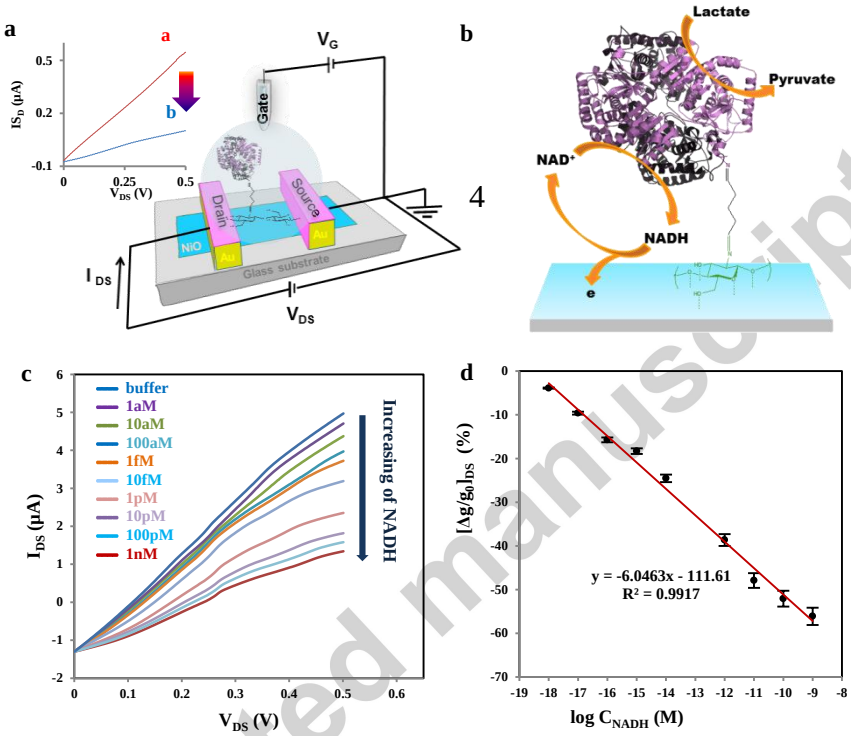

Fig.4

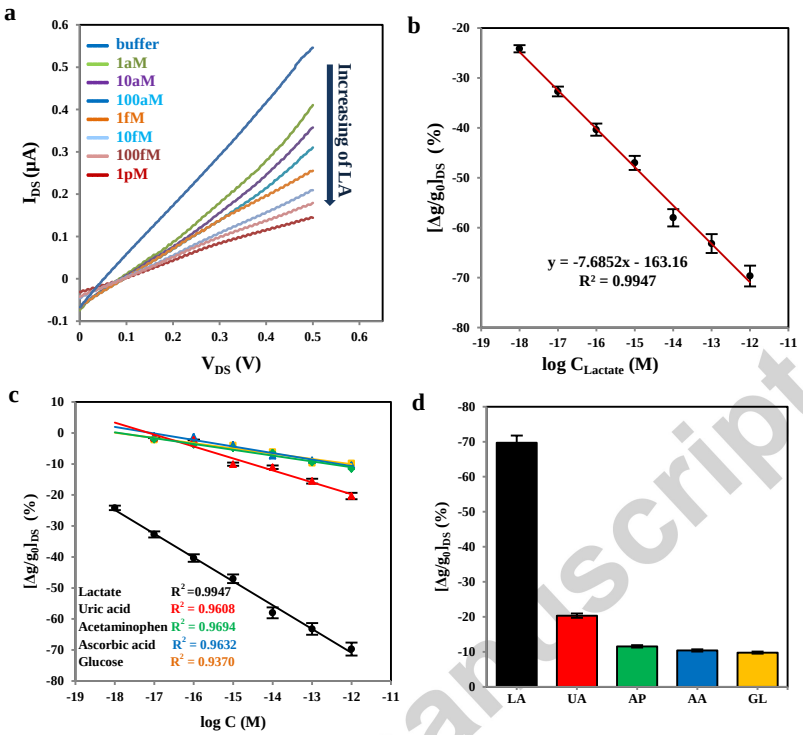

Fig.5